URSI GASS 2020, Rome, Italy, 29 August - 5 September 2020

Comparison of Spatial Averaging Methods of *In Situ* Electric Field for Low-Frequency Magnetic Field Exposures

Yinliang Diao* (1,2), and Akimasa Hirata(1,3)
(1) Department of Electrical and Mechanical Engineering, Nagoya Institute of Technology, Nagoya 466-8555, Japan
(2) College of Electronic Engineering, South China Agricultural University, Guangzhou 510642, China
(3) Center of Biomedical Physics and Information Technology, Nagoya Institute of Technology, Nagoya, 466-8555, Japan

Abstract

In the low-frequency (LF) electromagnetic dosimetry, two spatial averaging methods, volume averaging and line averaging, have been prescribed by ICNIRP and IEEE. However, their detailed implementations have not been explicitly mentioned yet, particularly when the averaging volume/line straddling across tissue/tissue and air/tissue interfaces. In this present paper, a total of four spatial averaging methods (two for volume averaging and two for line averaging) are proposed and investigated. The influence of the air/tissue adjacent to the specific tissue on interest is also discussed by introducing the maximum allowed percentage of air/other tissue in the averaging volume/line. The result reveal that the percentile *in situ* electric fields for the four averaging methods are comparable, neither method is likely to cause a significant difference between ICNIRP and IEEE with respect to dose estimation. With a ~20-30% inclusion of air/other tissue in averaging, stable percentile values are observed for internal tissues for volume averaging, with less stability observed for line averaging.

1 Introduction

For human protection from the electromagnetic fields, World Health Organization (WHO) review the related research and summarize the scientific evidence in environmental health criteria. Then, the international guidelines/standards are developed to set the limits based on scientific evidence. There are two international standardization bodies mentioned in WHO documents: International Commission on Non-Ionizing Radiation Protection (ICNIRP) [1] and IEEE International Committee on Electromagnetic Safety (ICES) [2, 3].

In general, ICNIRP and IEEE aim to protect against magnetic-field-coupled stimulation of excitable tissue both in the central nervous system (CNS) and peripherally for low frequency electromagnetic exposure. Both guidelines specify not-to-be-exceeded *in situ* electric fields in target tissue for exposure to an external magnetic field. ICNIRP calls the *in situ* limit the basic restriction (BR), and IEEE's equivalent term is the dosimetric reference limit (DRL). The limits established for environmental exposures – reference levels (RL) for ICNIRP and exposure reference levels (ERL) for IEEE – are derived such that compliance with them assures that the BR and DRL are not exceeded. Despite this mutual similarity, their specific approaches and specific quantitative limits differ on a number of counts [4, 5]. In the IEEE C95.6 standard [3], the *in situ* electric field should be averaged over 5-mm line. In the standard, the relationship between *in situ* electric field and external magnetic field strengths is derived analytically assuming that the human shape is comprised of ellipsoids. Therefore, the detailed procedure on how to handle the computational data as post-processing is not mentioned. In the ICNIRP guideline [1], it is mentioned that "*ICNIRP recommends determining the induced electric field as a vector average of the electric field in a small contiguous tissue volume of 2×2×2 mm^3. For a specific tissue, the 99th percentile value of the electric field is the relevant value to be compared with the basic restriction.*" The ambiguity of this description has been mentioned in the research agenda by IEEE ICES [4]. Then, several working groups are established to resolve related issues [6–7].

In our previous work [8], two spatial averaging methods have been investigated, with consideration of the cases where the averaging volume/line straddles a tissue/tissue or tissue/air interface. In [8], spatial averaging is performed only over the voxels belonging to the same targeted tissue in the averaging dimensions. In this paper, two additional spatial averaging methods are proposed and investigated. Then the differences in percentile *in situ* electric fields between averaging methods and the influence of the adjacent air/tissue beyond the tissue boundary are investigated using anatomical human models with different spatial resolutions.

2 Models and Methods

2.1 Electromagnetic Analysis

At frequencies up to ~10 MHz, the human body is assumed to not perturb the external magnetic field [9]. The Maxwell's equations can then be simplified with the quasi-static approximation by ignoring propagation, capacitive, and inductive effects. The resulting electric scalar potentials for an external magnetic field are computed using the scalar-potential finite-difference method by solving the following equation:

$$\nabla \cdot [\sigma(-\nabla\varphi - \mathrm{j}\omega \boldsymbol{A}_0)] = 0, \quad (1)$$

with boundary condition: $\mathbf{n} \cdot (\nabla\varphi + \mathrm{j}\omega \boldsymbol{A}_0) = 0$, where $\boldsymbol{A}_0$ and σ denote the magnetic vector potential of the applied magnetic field and the tissue conductivity, respectively. Scalar potential φ is computed by multigrid method. The *in situ* electric field $\boldsymbol{E}$ is calculated as: $\boldsymbol{E} = -\nabla\varphi - \mathrm{j}\omega \boldsymbol{A}_0$.

The Japanese adult male model TARO with spatial resolutions of 1 mm and 0.5 mm are adopted. The dielectric properties of human tissues are adopted from [10]. The exposure scenario considered here is a 50 Hz, 0.1 mT uniform magnetic field oriented in the anterior-posterior (AP) vector direction.

2.2 Spatial Averaging Methods

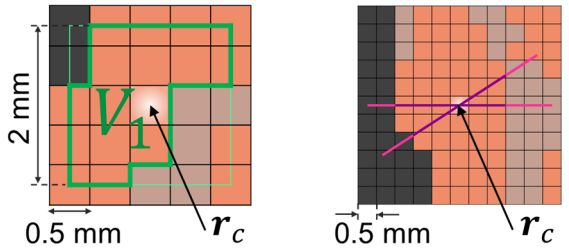

(a) (b)

Figure 1. Demonstration of (a) 2-mm cubic averaging, and (b) 5-mm linear averaging. Voxels with different colors represent different tissues.

A scheme for performing the volume averaging has been proposed in [8]. It will be first briefly recalled here for readers' convenience. Figure 1 (a) illustrates electric field averaging over a 2-mm cube for 0.5 mm resolution. The volume averaged *in situ* electric field, $E_V(\boldsymbol{r}_c)$, is evaluated as the arithmetic average of the vector electric field in the targeted tissue voxels in a 2-mm cube, and then assigned to the center voxel at $\boldsymbol{r}_c$. The volume of the targeted contiguous tissue inside the 2-mm cube is denoted by V_1 (outlined in thick green polygon). A factor p that represents the volume percentage of air/other tissues inside the 2-mm cube is defined as $p = 100 \times (V - V_1)/V$, where V = 8 mm^3. $p_{\max}$ is the maximum permissible percentage of air/other tissues in the cube. The averaging within target tissue ($r \in V_1$) is performed using (2).

$$E_V(\boldsymbol{r}_c) = \begin{cases} \dfrac{1}{V_1}\left\|\displaystyle\sum_{\boldsymbol{r}\in V_1} v(\boldsymbol{r})E(\boldsymbol{r})\right\| & \text{if } p < p_{\max} \\ 0\ \mathrm{V/m} & \text{otherwise} \end{cases} \quad (2)$$

where $\boldsymbol{r}_c$ is the location of the cube center, $v(\boldsymbol{r})$ is the intersected volume of the 2-mm cube with the voxel centered at $\boldsymbol{r}(\boldsymbol{r} \in V_1)$. The volume-averaging is applied to all voxels each centered in their respective cubes.

In (2), spatial averaging is performed over the voxels belonging to the same specific tissue. Therefore, if $p >$ 0%, the effective averaging volume V_1 will be smaller than 8 mm^3. In this paper, another volume averaging method as defined by (3) is also adopted. In (3), the electric field is averaged over all voxels within the 2-mm cube, if $p < p_{\max}$. Thus, the effective averaging volume maintains 8 mm^3.

$$E_V(\boldsymbol{r}_c) = \begin{cases} \dfrac{1}{V}\left\|\displaystyle\sum_{\boldsymbol{r}\in V} v(\boldsymbol{r})E(\boldsymbol{r})\right\| & \text{if } p < p_{\max} \\ 0\ \mathrm{V/m} & \text{otherwise} \end{cases} \quad (3)$$

The scheme for evaluating 5-mm linear averaging for a targeted voxel at $\boldsymbol{r}_c$ is illustrated in Figure 1 (b), in which 5-mm averaging lines are centered at the target voxel at $\boldsymbol{r}_c$, with the line's direction denoted by (θ, ϕ). The ratio of air/other tissues is defined as $p = 100 \times (L - L_1)/L$, where L_1 is the length of the segment within the same tissue (illustrated in dark magenta), and L = 5 mm. The linear averaging is performed using (4).

$$E_L(\boldsymbol{r}_c) = \begin{cases} \max\left(\dfrac{1}{L_1}\left\|\displaystyle\sum_{\boldsymbol{r}\in L_1} l(\boldsymbol{r})\boldsymbol{E}(\boldsymbol{r})\right\|\right) & \text{if } p < p_{\max} \\ 0\ \mathrm{V/m} & \text{otherwise} \end{cases} \quad (4)$$

where $l(\boldsymbol{r})$ is the length of the intersected segment of the 5-mm line with the voxel centered at $\boldsymbol{r}$. The directions of the averaging line (θ, ϕ) vary from 0° to 180° in 20° intervals. The final averaged value is taken as the maximum value over all directions. An additional line-averaging method defined by (5) is also adopted, in which the electric field is averaged over the entire 5-mm line segment, provided that $p < p_{\max}$. The four averaging methods adopted in this paper are summarized in Table 1.

$$E_L(\boldsymbol{r}_c) = \begin{cases} \max\left(\dfrac{1}{L}\left\|\displaystyle\sum_{\boldsymbol{r}\in L} l(\boldsymbol{r})\boldsymbol{E}(\boldsymbol{r})\right\|\right) & \text{if } p < p_{\max} \\ 0\ \mathrm{V/m} & \text{otherwise} \end{cases} \quad (5)$$

Table 1. Summary of Spatial Averaging Methods

No.	Type	Effective Averaging Volume/Line	No. of Tissues Included
1	Volume	V_1	1
2		V	≥ 1
3	Line	L_1	1
4		L	≥ 1

The relative difference in the averaged electric field between two averaging methods is defined as:

$$d_{i,j} = 100 \times \frac{|E_i - E_j|}{E_{\mathrm{ref}}} \quad (6)$$

where E_i and E_j are averaged electric field using method i and j, respectively, $i,j \in \{1,2,3,4\}$, the reference value, E_{ref}, is the mean of E_i and E_j.

3 Results

3.1 Percentile Values of Averaged Electric Fields

The top 1% of the *in situ* electric field strengths in TARO evaluated using the four averaging methods are listed in Table 2, for $p_{\max} = 40\%$. In general, excluding the top ~0.1% voxels, the averaged electric fields calculated using the four averaging methods are comparable. The relative differences, $d_{1,2}$ and $d_{3,4}$, are within ~7%, excluding the maximum (the 100$^{\text{th}}$ percentile value). If the highest 1% electric fields are excluded, $d_{1,2}$ and $d_{3,4}$ decrease to 0.97% and 1.0% for muscle, and decrease to 0.2% and 1.63% for grey matter, respectively. The relative differences between volume and line averaging, $d_{1,3}$ and $d_{2,4}$, for the 99$^{\text{th}}$ percentile values are also within ~2% for muscle and grey matter. Slightly large relative differences between volume and line averaging, $d_{1,3}$ and $d_{2,4}$, can be observed for skin ($d_{2,4}$=7.91% for 99.9$^{\text{th}}$ percentile value). This is because the sets of averaged voxels are different, tissues like the skin are too thin to cover the whole averaging cube, while the averaging line can be orientated such that the segment is still located within the thin tissue.

Table 2. Relative Differences in Percentile Values of *In Situ* Electric Field Strength in Selected Tissues

Tissue	%ile	$d_{1,2}$	$d_{3,4}$	$d_{1,3}$	$d_{2,4}$
All tissues	100	3.53	1.13	0.66	1.74
	99.99	3.39	4.95	1.14	2.70
	99.9	4.20	3.64	2.83	2.27
	99	1.70	1.39	0.89	0.58
Skin	100	3.53	1.13	0.66	1.74
	99.99	2.77	3.90	5.28	6.41
	99.9	0.38	1.76	6.53	7.91
	99	1.17	0.03	1.24	2.43
Muscle	100	7.42	1.54	4.85	1.04
	99.99	4.03	3.65	0.15	0.23
	99.9	2.18	2.20	0.34	0.32
	99	0.97	1.00	0.38	0.35
Grey Matter	100	14.11	12.85	9.94	17.02
	99.99	3.76	6.76	1.29	4.29
	99.9	1.06	3.71	0.11	2.76
	99	0.20	1.63	0.18	1.25

3.2 Effect of Model Resolution

The effect of the model resolution on the percentile values of averaged *in situ* electric fields are investigated using TARO model with resolutions of 1 mm and 0.5 mm. The top 1% of the averaged *in situ* electric field strengths in TARO are shown in Figure 2, for different tissues. To avoid redundancy, only the averaging methods 1 and 3 are compared in the figure. In general, the higher resolution model provides higher electric field strengths for anatomical models. Excluding the maximum, the volume- and line-averaged values are rather stable for different model resolutions.

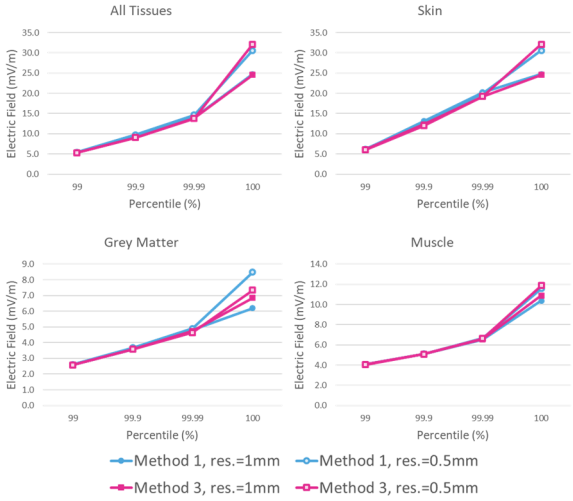

Figure. 2. Percentile values of averaged *in situ* electric field in selected tissues of TARO with different spatial resolutions, $p_{\max} = 40\%$.

3.3 Effect of $p_{\max}$

The averaged *in situ* electric fields for different percentages of air/other tissues inclusion in the cube and line are also investigated. Figure 3 shows the *in situ* electric field strengths for different $p_{\max}$ values for selected tissues of TARO model. A value of $p_{\max}$ = 0% produces the lowest averaged *in situ* electric field. As $p_{\max}$ increases in steps of 10%, the percentile values increase.

In general, if $p_{\max}$>20-30%, reproducible percentile values can be expected for internal tissues for volume averaging. For the line averaging, the curves appear slightly more sensitive to $p_{\max}$ and tissue types, as can be seen from the results. For relatively thin tissues such as skin, unstable percentile values are observed for the two volume averaging methods. In contrast, the 99$^{\text{th}}$ percentile values of the line-averaged fields are stable for skin.

4. Discussion and Concluding Remarks

Volume- and line- averaging of *in situ* electric field in human body have been prescribed by ICNIRP and IEEE, respectively. However, neither guideline/standard provides further guidance as to specific dosimetric procedures for assessing compliance with the BR or DRL. In our previous work, volume and line averaging methods (method 1 and 3) have been implemented, however, only the voxels or line segments belonging to the same target tissue are included in averaging. To maintain a fixed averaging volume/length, two additional methods (method 2 and 4) are proposed and investigated in this paper, where all the voxels inside the 2-mm cube or 5-mm line are included in spatial averaging.

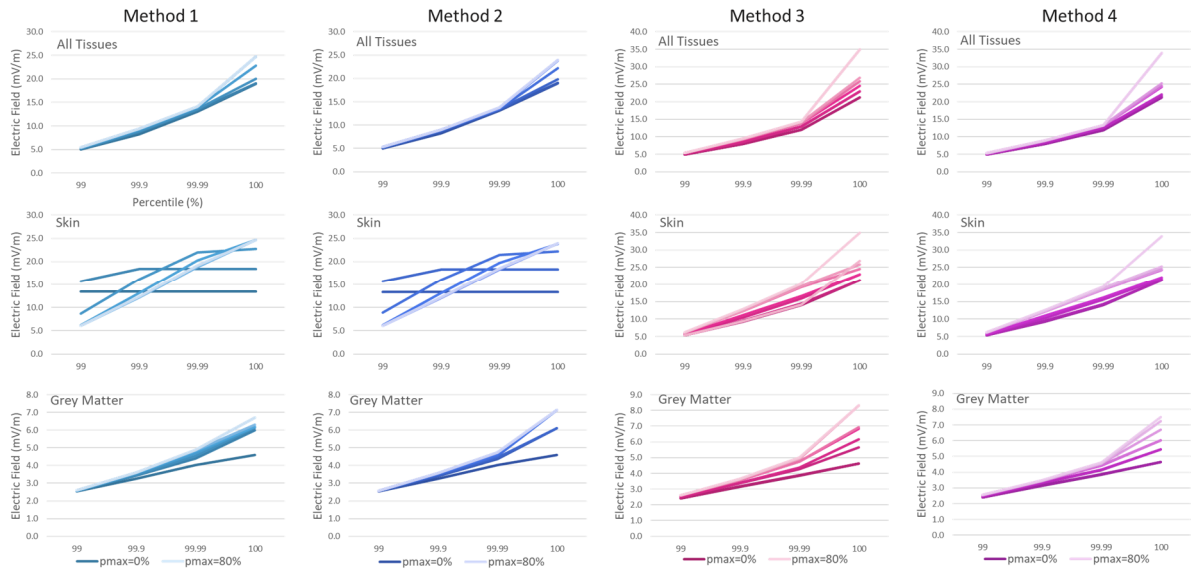

Figure 3. Percentile values of averaged *in situ* electric field in selected tissues of TARO (res.=1 mm) for different p_{max}.

The analyses presented here compared the *in situ* electric fields between the four averaging methods when the averaging volume/line falls entirely within the specific target tissue, and when it is extended to tissue boundary. For the ≤99.99th percentile of inner tissues, good agreement is found in the *in situ* electric field between different averaging methods, with relatively large differences for maximum values (100th percentile). Although volume- and line- averaging probably relate to different *in situ* electric field interactions, the dosimetry results for the four averaging methods indicate that their percentile *in situ* electric fields are not radically different from one another. Thus, neither scheme is likely to cause a significant difference between ICNIRP and IEEE with respect to dose estimation.

5 Acknowledgements

This work was supported in part by the Ministry of Internal Affairs and Communications, Japan.

6 References

1. International Commission on Non-Ionizing Radiation Protection, "Guidelines for Limiting Exposure to Time-Varying Electric and Magnetic Fields (1 Hz to 100 kHz).," *Health Phys.*, **99**, 6, pp. 818–36, 2010.

2. IEEE-C95.1, IEEE Standard for Safety Levels with Respect to Human Exposure to Electric, Magnetic and Electromagnetic Fields, 0 Hz to 300 GHz. NY, USA, 2019.

3. IEEE-C95.6, IEEE Standard for Safety Levels with Respect to Human Exposure to Electromagnetic Fields, 0 to 3 KHz. NY, USA, 2002.

4. J. P. Reilly and A. Hirata, "Low-Frequency Electrical Dosimetry: Research Agenda of the IEEE International Committee on Electromagnetic Safety," *Phys. Med. Biol.*, **61**, 12, p. R138, 2016.

5. X. Chen et al., "Analysis of Human Brain Exposure to Low-Frequency Magnetic Fields: A Numerical Assessment of Spatially Averaged Electric Fields and Exposure Limits," *Bioelectromagnetics*, **34**, 1, pp. 375–384, 2013.

6. D. Poljak et al., "On the Use of Conformal Models and Methods in Dosimetry for Nonuniform Field Exposure," *IEEE Trans. Electromagn. Compat.*, **60**, 2, pp. 328-337, 2018.

7. J. Gomez-Tames, I. Laakso, Y. Haba, A. Hirata, D. Poljak, and K. Yamazaki, "Computational Artifacts of the *In Situ* Electric Field in Anatomical Models Exposed to Low-Frequency Magnetic Field," *IEEE Trans. Electromagn. Compat.*, **60**, 3, pp. 589-597, 2018.

8. Y. Diao, J. Gomez-Tames, E. A. Rashed, R. Kavet, and A. Hirata, "Spatial Averaging Schemes of *In Situ* Electric Field for Low-Frequency Magnetic Field Exposures," *IEEE Access*, **7**, pp. 184320–184331, 2019.

9. A. Hirata, F. Ito, and I. Laakso, "Confirmation of Quasi-Static Approximation in SAR Evaluation for a Wireless Power Transfer System.," *Phys. Med. Biol.*, **58**, 17, pp. N241-249, 2013.

10. S. Gabriel, R. W. Lau, and C. Gabriel, "The Dielectric Properties of Biological Tissues: III. Parametric Models for The Dielectric Spectrum of Tissues," *Phys. Med. Biol.*, **41**, 11, pp. 2271–2293, 1996.